

The measurement by SAXS of the nematic order parameter of laponite gels

B. J. LEMAIRE¹, P. PANINE², J. C. P. GABRIEL^{3,4} and P. DAVIDSON¹(*)

¹ *Laboratoire de Physique des Solides, UMR CNRS 8502*

Bâtiment 510, Université Paris-Sud - 91405 Orsay, France

² *European Synchrotron Radiation Facility - BP 220, 38043 Grenoble, France*

³ *Sciences Moléculaires aux Interfaces, FRE CNRS 2068*

2 rue de la Houssinière, BP 32229, 44322 Nantes, France

⁴ *Nanomix Inc. - 1295 A 67th Street, CA 94608, Emeryville, USA*

(received 28 January 2002; accepted in final form 15 April 2002)

PACS. 61.10.-i – X-ray diffraction and scattering.

PACS. 61.30.-v – Liquid crystals.

PACS. 82.70.-y – Disperse systems; complex fluids.

Abstract. – We performed small-angle X-ray scattering (SAXS) experiments on oriented samples of laponite clay gels obtained by slow evaporation. The SAXS patterns are clearly anisotropic, which demonstrates the existence of nematic-like orientational correlations of the laponite disc-like particles. The iso-intensity lines of the SAXS patterns are elliptical and roughly homothetic over the whole scattering vector range examined in this experiment. The value of the nematic order parameter, $S = 0.55 \pm 0.05$, derived from the SAXS patterns is comparable to that of usual liquid crystals. This large value proves the importance of orientational correlations in these gels at concentrations higher than $0.02 \text{ g} \cdot \text{cm}^{-3}$, even in the absence of shear.

Introduction. – Laponite clay suspensions have recently attracted wide attention due not only to their widespread industrial applications but also, from a more fundamental point of view, to the fact that they form a gel phase, the nature of which is not yet fully understood [1–8]. Laponite particles are disc-like moieties of approximately $L = 1 \text{ nm}$ thickness and $R = 15 \text{ nm}$ radius that can easily be dispersed in water to produce visco-elastic suspensions stable at $\text{pH} \geq 9$ [3]. Electron microscopy images of these suspensions [3] have shown that the clay particles are not in contact, which strongly disagrees with the “house of cards” structure that was suggested long ago for the organisation of these gels [1]. In the last few years, the origin of the gelation has been a subject of intense debate, but has still remained elusive. Nevertheless, it appears that a significant feature of laponite particles is their surface electric charge, giving rise to electrostatic interactions that may play a major role in the phenomenon. In this context, the observation by polarised light microscopy of nematic-like textures in these materials provides a complementary perspective. As early as 1938, I. Langmuir detected birefringence in suspensions of bentonite, another smectite clay of the same family as laponite [9].

(*) E-mail: davidson@lps.u-psud.fr

More recently, detailed optical observations of laponite suspensions have demonstrated the existence of two distinct transitions as the concentration increases [10]. At low concentration, laponite suspensions are isotropic (I) liquids; beyond a concentration called $c_g \approx 0.01 \text{ g} \cdot \text{cm}^{-3}$, the suspensions form isotropic gels; beyond another concentration called $c_{N/I} \approx 0.02 \text{ g} \cdot \text{cm}^{-3}$, the gels become birefringent. This birefringence suggests that these materials may belong to the broad class of lyotropic liquid crystals. Indeed, in spite of their elastic and aging properties, clay gels can be compared with nematic (N) suspensions of anisotropic rigid colloidal particles such as those of stiff rod-like polymers [11]. Actually, it is now well established that colloidal suspensions of mineral moieties can form liquid crystalline phases [12]. However, even though the birefringence and optical textures strongly suggest, qualitatively speaking, the existence of nematic orientational order in these gels, this order remains to be quantitatively evaluated. The purpose of the present work is therefore to measure the nematic order parameter, S , of these materials (S takes values between 0 for randomly oriented particles and 1 for perfectly aligned particles) [11]. Indeed, the relevance of nematic correlations to the gel description will of course depend on the magnitude of S . A small S value (10^{-3} – 10^{-2}) would rather suggest that the gel birefringence is not an important phenomenon, which possibly arises from sample preparation, and is therefore purely extrinsic. In contrast, an S value in the usual range (0.3–0.8) for liquid crystals would demonstrate the significance of orientational correlations.

The nematic order parameter can be measured by scattering techniques (X-rays and neutrons), but this requires the preparation of a single domain sample. Considering previous studies of laponite suspensions [13–18], X-ray scattering seems appropriate because of the good contrast between clay particles and water, but the scattering takes place at small angles due to the particle size. Therefore, we describe here the preparation of well-oriented laponite gel samples and their investigation by small-angle X-ray scattering (SAXS). Moreover, we calculate here the nematic order parameter of an assembly of disks (or cylinders) with no positional correlations from its X-ray scattering pattern.

Experimental. – Gels of laponite B (a synthetic microcrystalline clay of hectorite type, manufactured by Laporte, Ltd.) were prepared using the following procedure. 1% w/w laponite clay was dispersed into 18 M Ω water ($p\text{H} = 6$), and stirred vigorously for at least 24 h. The suspensions obtained were centrifuged at 2000 rpm for 6 h and only the top fraction was kept, leading to ca. 1% w/w colourless completely transparent homogeneous fluids. The concentrations of these suspensions were determined from weight loss measured after drying at 160 °C. Stock samples were held under argon atmosphere to avoid CO₂ dissolution, which allowed to keep their $p\text{H}$ between 8 and 9 and to prevent clay dissolution and flocculation.

Aligned samples of laponite gels must be produced in order to measure the nematic order parameter by SAXS. We previously obtained highly aligned samples by letting isotropic ($c = 0.016 \text{ g} \cdot \text{cm}^{-3}$) suspensions concentrate slowly by evaporation, over a few months, in test tubes of 1 cm diameter [10]. However, these aligned samples are not suitable for X-ray scattering because of their size and the glass wall thickness. Therefore, we had to scale down this alignment technique to samples held in Lindemann glass capillary tubes of 1.5 mm diameter. This introduced new problems because the suspensions strongly wet the capillary walls, leaving the clay material as a thin coating on the glass surface. In order to avoid this effect, the capillaries were hydrophobically treated in the following way. A metal plate was placed over a Petri dish so as to form a tight container. The tips of the capillaries to be treated were carefully broken to open them at both ends. They were set vertically upside-down with their funnels tightly adjusted to holes bored through the metal plate. This ensemble (Petri dish, metal plate and capillaries) was placed in an oven at 120 °C for an hour, and then in a hood at room temperature. 30 μL of N,N-dimethyltrimethylsilylamine

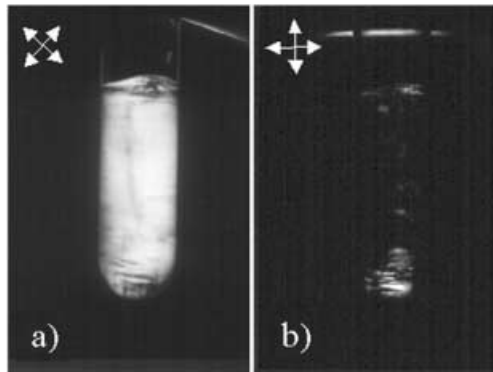


Fig. 1

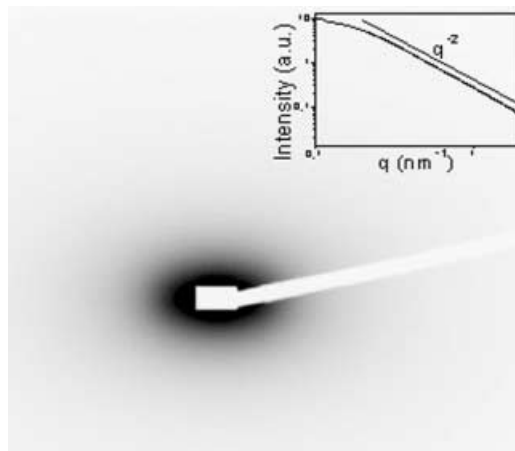


Fig. 2

Fig. 1 – Optical textures observed in polarized light of an aligned sample of clay gel in an X-ray capillary. a) Maximum transmission; the capillary axis makes an angle of 45° with the directions of the polariser and the analyser. b) Extinction; the capillary axis is parallel to the directions of the polariser or the analyser.

Fig. 2 – Anisotropic SAXS pattern of an aligned sample of clay gel in a horizontal capillary. Insert: SAXS intensity *vs.* scattering vector modulus of an unoriented sample of the same concentration. (The straight line shows the q^{-2} -dependence typical of the “intermediate regime” of plate-like particles in a log-log representation.)

(DMTSA, $(\text{CH}_3)_3\text{SiN}(\text{CH}_3)_2$ Fluka) were injected in the Petri dish and allowed to evaporate through the capillaries for about 10 minutes under the hood. Finally, the capillaries were placed back in the oven at 120°C for another hour. This procedure efficiently avoided the wetting problems mentioned above. A number of treated capillaries were filled with $50\ \mu\text{L}$ of an isotropic laponite suspension ($c = 0.01\ \text{g} \cdot \text{cm}^{-3}$); they were left to dry slowly at 40°C over two weeks until their concentration reached $c \approx 0.03\ \text{g} \cdot \text{cm}^{-3}$. The capillaries were then carefully flame-sealed.

The SAXS measurements were performed at the high-brilliance beamline (ID2) at the European Synchrotron Radiation Facility in Grenoble, France. The pinhole camera setup and standard procedure for data acquisition and treatment are described elsewhere [19]. The beam size at the sample position was about $0.1 \times 0.1\ \text{mm}^2$. The 2-dimensional SAXS patterns were acquired using an image intensified CCD detector. The incident wavelength (λ) was $0.0995\ \text{nm}$ and the sample-to-detector distance was either $3\ \text{m}$ or $10\ \text{m}$. This combination provided a useful range of scattering vector (\vec{q}) modulus of $0.02\ \text{nm}^{-1} \leq q \leq 0.6\ \text{nm}^{-1}$ or $1\ \text{nm}^{-1} \leq q \leq 2\ \text{nm}^{-1}$. Here, q is given by $q = \frac{4\pi}{\lambda} \sin \theta$, where 2θ is the scattering angle.

Results. – Figure 1 shows the optical textures (between crossed polarisers) of the slowly concentrated samples held in Lindemann glass capillaries. These samples are fairly well aligned, as they appear uniformly dark when the capillary axis is parallel to the polariser direction and bright when the capillary axis is oriented at 45° . Qualitatively speaking, it should be noted that the birefringence is large enough to be very easily observed, which already suggests an appreciable orientation of the particles.

The SAXS pattern of an oriented sample of clay gel is displayed in fig. 2 where an anisotropic diffuse spot can be seen around the beam trap. The sample-detector distance

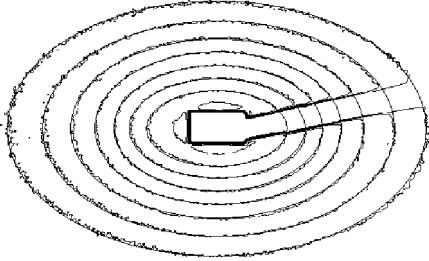


Fig. 3

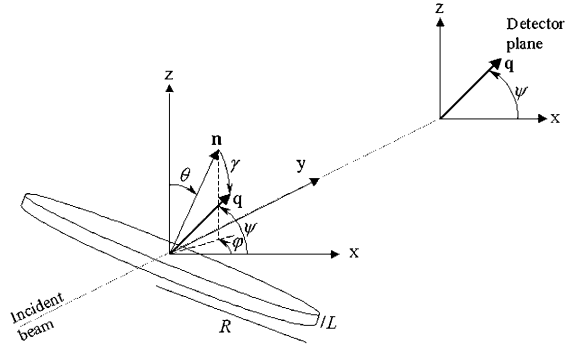


Fig. 4

Fig. 3 – Iso-intensity lines of the SAXS pattern in fig. 2. These experimental iso-intensity lines are well described by ellipses (thin solid lines).

Fig. 4 – Geometry of the scattering experiment that shows the definitions of the angular coordinates referred to in the text.

was 3 m. The diffuse spot is more extended along the horizontal direction, which implies that the thin clay particles are vertical. Since the capillary axis was set horizontal, this means that, on average, the clay particles have their normal aligned along the capillary axis, possibly due to the influence of the free surface of the sample.

The scattered intensity I of the diffuse spot regularly decreases with q as q^{-2} (fig. 2 insert), which is typical of the form factor of plate-like particles in the so-called "intermediate regime" ($\frac{2\pi}{R} \leq q \leq \frac{2\pi}{L}$) [20]. Therefore, inter-particle positional correlations are completely negligible in this q range. This is not at all surprising in the light of previous work that repeatedly reported on the weakness of positional correlations in such systems [3, 13, 14].

The iso-intensity lines (fig. 3) derived from the SAXS pattern are well approximated by concentric ellipses that are roughly homothetic. The ratios $\frac{a}{b}$ of the long axis a to the short axis b of these ellipses range from 1.85 to 1.65. The iso-intensity lines located at higher angles, that correspond to weaker scattered intensity, are less anisotropic. Because of their weaker intensity, they may be affected by the isotropic background noise, which is mostly due to the CCD camera.

The SAXS patterns recorded at 10 m are also markedly anisotropic and quite similar. Their iso-intensity lines are elliptical with $\frac{a}{b} \approx 1.75 \pm 0.10$. Therefore, the same experimental results were found in the whole q range explored. We now need to derive the nematic order parameter S from this scattering data.

Discussion. – The derivation of orientational distribution functions from scattering data is generally complicated by the coupling between the orientational and positional orders of the scattering moieties. In the field of liquid crystals, S is usually calculated either by considering single-molecule (neutron) scattering, so that positional correlations are irrelevant, or by assuming ideal positional correlations within a small group of molecules. The situation here is actually much simplified by the absence of positional correlations in the q range probed. Then, the scattering can be analysed only in terms of the particle form factor and the orientational distribution function.

In the following analysis of the scattering, we adopt notations similar to those of Hayter and Penfold [16, 21] in their treatment of a closely related problem (fig. 4). The form factor

of a cylinder of height L and radius R is classically [20] given by

$$F(q, \gamma) = K \frac{\sin(qL \cos \gamma)}{qL \cos \gamma} \frac{J_1(qR \sin \gamma)}{qR \sin \gamma}, \quad (1)$$

where K is a constant that includes the electron density contrast between the particles and the solvent, J_1 is the first-order Bessel function and γ is the angle between the cylinder axis \vec{n} and \vec{q} . We call θ and ϕ the polar and azimuthal angles of the cylinder axis \vec{n} in a system of coordinates where the z -axis is taken along the nematic director and the y -axis along the incident X-ray beam. We call ψ the angle between \vec{q} and the x -axis (fig. 4). These angles are then related by

$$\cos \gamma = \cos \theta \sin \psi + \sin \theta \cos \psi \cos \phi. \quad (2)$$

In contrast with previous work, we now explicitly introduce the Maier-Saupe orientational distribution function which is most commonly used in the field of liquid crystals [11, 22]:

$$f(\theta) = \frac{1}{Z} \exp[m \cos^2 \theta], \quad (3)$$

where Z is a normalisation constant and m is the Maier-Saupe distribution parameter that is directly related to S [22]. Averaging the form factor with the use of this distribution function directly gives the scattered intensity

$$I(\vec{q}) = I(q, \psi) = 2K^2 \int_0^{2\pi} d\phi \int_0^{\frac{\pi}{2}} f(\theta) F^2(q, \gamma) \sin \theta d\theta. \quad (4)$$

The theoretical SAXS pattern predicted by this formula was calculated using the software MATHEMATICA [23] and compared with the experimental one in order to extract S . Let us note here that this analysis should apply to any nematic suspension of cylindrical moieties, provided that inter-particle positional correlations are negligible and that the Maier-Saupe distribution function is obeyed.

As can be seen from fig. 5, the theoretical pattern is indeed anisotropic and the predicted iso-intensity lines look roughly elliptical. Good agreement with the experimental iso-intensity lines is found for $S = 0.55 \pm 0.05$. It should be noted that the particle dimensions have only limited influence on the theoretical scattering pattern. The plate thickness, L , may vary from 0.5 to 2 nm and its radius, R , from 10 to 25 nm without altering the value of S within the 0.05 error bars. In contrast, the scattering pattern anisotropy is very sensitive to the value of S , which allows us to obtain its value fairly accurately.

At this point, let us reconsider the optical properties of the laponite clay gels. In fact, at such concentrations ($0.03 \text{ g} \cdot \text{cm}^{-3}$), the birefringence of samples held in flat glass (untreated) capillaries is easily observed with no special experimental care. Using the approximate relation $e\Delta n \approx \lambda_{\text{opt}}/10$ for the birefringence detection limit of our crude apparatus (with $e = 50 \text{ } \mu\text{m}$ the capillary thickness and $\lambda_{\text{opt}} \approx 0.5 \text{ } \mu\text{m}$ the wavelength of visible light) gives us an order of magnitude for the birefringence of the suspensions, $\Delta n \approx 10^{-3}$, that is in good agreement with previous experimental studies [24]. Now, the birefringence of the suspension may also classically be written $\Delta n \approx \Delta n_{\text{sat}} \phi S$, where ϕ is the volume fraction ($\phi \approx 10^{-2}$) and Δn_{sat} is the particle birefringence that is mostly due to form birefringence ($\Delta n_{\text{sat}} \approx 0.1$). This gives us a value, $S \approx 1$, of the same order of magnitude as that measured by SAXS. Therefore, this rough reasoning shows us that the gel birefringence and SAXS pattern anisotropy are indeed two aspects of the same orientational ordering phenomenon.

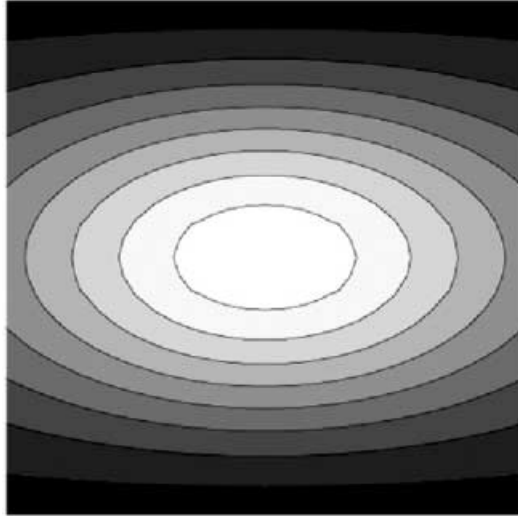


Fig. 5 – Calculation of the SAXS pattern, using the procedure described in the text, with $L = 1$ nm, $R = 15$ nm and $S = 0.55$, that gives good agreement with the experimental one (figs. 2, 3).

Both the birefringence and the SAXS anisotropy suggest the existence of nematic ordering. In fact, the Onsager model and numerical simulations of assemblies of plate-like particles [25–27] predict a first-order phase transition from the isotropic phase to a nematic one as concentration increases. The value of S at the transition should be around 0.7-0.8 whereas we derived a value of S somewhat smaller. This may simply be due to the fact that some topological defects still remain in our oriented samples grown by slow evaporation. Indeed, the measurement by X-ray scattering of S for usual liquid crystals generally involves the use of a magnetic field to fully eliminate topological defects and completely align the sample. However, due to their strong elastic properties, clay gels are not very likely to be oriented in this way. More generally, the gel character of these suspensions prevents the observation of the classical properties of nematic phases, such as fluidity and phase separation at the onset of the orientational ordering. However, we note that the birefringence of these materials appears at about the same concentration for samples very slowly concentrated over months, thus undergoing negligible shear rates, and for samples directly mixed in test tubes, under vigorous stirring. This means that the orientational correlations arising at concentrations beyond $\approx 0.02 \text{ g} \cdot \text{cm}^{-3}$, being independent of the sample preparation, are intrinsic. Finally, this nematic-like description of clay gels drawn from the SAXS pattern clearly contradicts the old “house of cards” model, at least in these concentration and ionic ranges, as did other recent experimental investigations on the same or similar clay gels [3, 14, 18, 28, 29].

Conclusion. – The SAXS pattern of oriented samples of clay gels is quite anisotropic. The value of the nematic order parameter that we obtained, $S = 0.55 \pm 0.05$, is comparable to those of usual liquid crystals. This experiment, therefore, illustrates the magnitude of orientational correlations between clay particles in laponite gels, even in the absence of shear. These correlations can extend over centimetres since large ($\approx 1 \text{ cm}^3$) macroscopically oriented samples can readily be prepared in test tubes by slow evaporation [10]. This long-range orientational order could be exploited when preparing clay-based materials such as pillared-clay catalysts and clay-polymer composites. Moreover, we stress that nematic-like orientational

correlations should always be kept in mind when elaborating experimental procedures and should also be included in any thorough theoretical description of these puzzling clay gels.

* * *

We are deeply indebted to M. LEONETTI for showing us the hydrophobic treatment of the X-ray capillary tubes and to ESRF for the award of beamtime SC725. BL gratefully acknowledges financial support from the Ecole Normale Supérieure and the Ecole Nationale des Ponts et Chaussées.

REFERENCES

- [1] VAN OLPHEN H., *Faraday Discuss. Chem. Soc.*, **11** (1951) 82.
- [2] NORRISH K., *Faraday Discuss. Chem. Soc.*, **18** (1954) 120.
- [3] MOURCHID A. *et al.*, *Langmuir*, **11** (1995) 1942; **14** (1998) 4718; MOURCHID A. and LEVITZ P., *Phys. Rev. E*, **57** (1998) R4887; LEVITZ P. *et al.*, *Europhys. Lett.*, **49** (2000) 672; COUSIN F., CABUIL V. and LEVITZ P., *Langmuir*, **18** (2002) 1466.
- [4] DIJKSTRA M., HANSEN J. P. and MADDEN P. A., *Phys. Rev. Lett.*, **75** (1995) 2236.
- [5] PIGNON F., PIAU J. M. and MAGNIN A., *Phys. Rev. Lett.*, **76** (1996) 4857; PIGNON F., MAGNIN A. and PIAU J. M., *Phys. Rev. Lett.*, **79** (1997) 4689; PIGNON F. *et al.*, *Phys. Rev. E*, **56** (1997) 3281.
- [6] BONN D. *et al.*, *Europhys. Lett.*, **45** (1998) 52; *Langmuir*, **15** (1999) 7534.
- [7] RAMSAY J. D. F., *J. Colloid Interface Sci.*, **109** (1986) 441.
- [8] KROON M., WEGDAM G. H. and SPRIK R., *Phys. Rev. E*, **54** (1996) 6541.
- [9] LANGMUIR I., *J. Chem. Phys.*, **6** (1938) 873.
- [10] GABRIEL J. C. P., SANCHEZ C. and DAVIDSON P., *J. Phys. Chem.*, **100** (1996) 11139.
- [11] DE GENNES P. G., *The Physics of Liquid Crystals* (Clarendon Press, Oxford) 1979.
- [12] For a review, see GABRIEL J. C. P. and DAVIDSON P., *Adv. Mater.*, **12** (2000) 9; GABRIEL J. C. P. *et al.*, *Nature*, **413** (2001) 504.
- [13] MORVAN M., ESPINAT D., LAMBARD J. and ZEMB T., *Colloid Surf. A*, **82** (1994) 193.
- [14] SAUNDERS J. M. *et al.*, *J. Phys. Chem. B*, **103** (1999) 9211.
- [15] RAMSAY J. D. F. and LINDNER P., *J. Chem. Soc. Faraday Trans.*, **89** (1993) 4207.
- [16] RAMSAY J. D. F., SWANTON S. W. and BUNCE J., *J. Chem. Soc. Faraday Trans.*, **86** (1990) 3919.
- [17] CLARKE S. M., RENNIE A. R. and COVERT P., *Europhys. Lett.*, **35** (1996) 233.
- [18] AVERY R. G. and RAMSAY J. D. F., *J. Colloid Interface Sci.*, **109** (1986) 448.
- [19] NARAYANAN T., DIAT O. and BOESECKE P., *Nucl. Instrum. Methods Phys. Res.*, **177** (2001) 1005.
- [20] GUINIER A. and FOURNET G., *Small Angle Scattering of X-rays* (Wiley, New York) 1955.
- [21] HAYTER J. B. and PENFOLD J., *J. Phys. Chem.*, **88** (1984) 4589.
- [22] MAIER W. and SAUPE A., *Z. Naturforsch. A*, **13** (1958) 564; **14** (1959) 882; **15** (1960) 287.
- [23] MATHEMATICA 4.0 SOFTWARE, Wolfram Research Inc. (<http://www.wolfram.com>).
- [24] PIGNON F. *et al.*, *J. Membrane Sci.*, **174** (2000) 189.
- [25] ONSAGER L., *Ann. N.Y. Acad. Sci.*, **51** (1949) 627.
- [26] FORSYTH P. A. *et al.*, *Adv. Colloid Interface Sci.*, **9** (1978) 37.
- [27] EPPENGA R. and FRENKEL D., *Mol. Phys.*, **52** (1984) 1303; FRENKEL D., *Liq. Cryst.*, **5** (1989) 929.
- [28] DIMASI E., FOSSUM J. O., GOG T. and VENKATARAMAN C., *Phys. Rev. E*, **64** (2001) 061704.
- [29] BIHANNIC I. *et al.*, *Langmuir*, **17** (2001) 4144.